

Title	Strain Steps and the Dislocation Fault Model
Author(s)	TAKEMOTO, Shuzo
Citation	Bulletin of the Disaster Prevention Research Institute (1970), 20(1): 1-15
Issue Date	1970-10
URL	http://hdl.handle.net/2433/124789
Right	
Type	Departmental Bulletin Paper
Textversion	publisher

Strain Steps and the Dislocation Fault Model

By SHUZO TAKEMOTO

(Manuscript received June 29, 1970)

Abstract

Strain steps associated with earthquakes ranging in magnitude from 3.2 to 7.9 have been observed at the Iwakura, Amagase and Donzurubo Observatories using super-invar bar extensometers. The stability of these instruments for vibration was confirmed by two methods.

The amplitude of strain step depends on distance proportionately with $R^{-2.4}$, and based on certain assumptions, fault length seems to be related to earthquake magnitude according to following formula:

$$M=2.2 \log L-8.4$$

where L is the fault length in cm.

Furthermore, observed values of strain steps associated with earthquakes of comparatively small magnitude ($M=3.2\sim 5.6$) occurring in the northern part of the Kinki district have been compared with the residual strain fields calculated by F. Press in 1965.

1. Introduction

The observational data of strain steps and other permanent deformations in the vicinity of faults caused by major earthquakes have been well explained by mathematical models of faulting based on the elasticity theory of dislocations.

Chinnery¹⁾, using the results of Steketee (1958), made contour maps of the displacement and stress fields in the vicinity of a vertical, rectangular, strike-slip fault and he applied these to the observed values of ground deformations produced by the Tango and North Izu earthquakes and to the San Andreas Fault.

Press²⁾ computed and contoured residual displacement, strain and tilt fields at teleseismic distance for vertical, rectangular, strike-slip and dip-slip faults. He also applied these contour maps to the strain step record made in Hawaii for the Alaska earthquake of 1964, and showed that the far-field residual strains caused by major earthquakes were large enough to be detected by modern instruments.

Wideman and Major³⁾, using the records of strain steps obtained at the Green Observatory and other supplemental geodetic survey data, proposed that their amplitude dependence upon distance could be expressed as $R^{-1.5}$.

In this paper, the data on strain steps obtained at our three observatories have been treated by the same methods used by Wideman and Major in regard to strain step amplitude dependence upon distance. Then, the near-field residual strains have been investigated in connection with the dislocation fault model in a semi-infinite elastic medium using the data from strain steps of earthquakes which occurred in the northern part of the Kinki district, earthquakes ranging in magnitude from 3.2 to 5.6, and as a result of which no visible seismic faulting appeared.

The treatment outlined above is practical for the following reasons:

(1) All the data of strain steps for earthquakes occurring in the northern part of the Kinki district, the so-called "Yodo River Seismically Active Zone" (Okano and

Hirano, 1968⁴⁾), have been obtained at observatories whose epicentral distances were shorter than 100 km, so that a half-space model can be used without considering the effect of the earth's curvature.

(2) The focal mechanisms of the earthquakes occurring in this region have been investigated in detail and the direction of maximum pressure of all these earthquakes shows a definite pattern which is independent of magnitude (Okano and Hirano⁵⁾, Hashizume et al.⁶⁾). This fact permits us to superpose the data of strain steps associated with these local earthquakes.

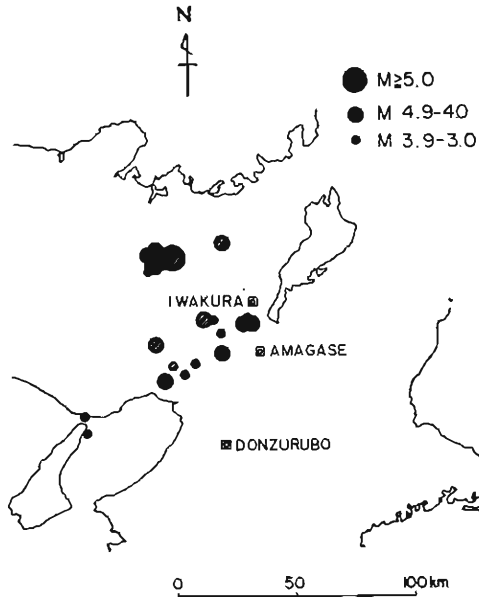


Fig. 1 Locations of observatories and epicenters of earthquakes listed in Table 2.

Table 1

Observatory	Mark	Direction	Sensitivity
Iwakura (35°05'N, 135°48'E)	E-1	N06°E	9.5×10^{-9} /mm
	E-2	E06°S	4.6 "
	E-3	E28°S	2.9 "
Amagase (34°53'N, 135°50'E)	E-1	N68°W	6.1×10^{-9} /mm
	R-2	N67°E	3.8×10^{-8} /mm
	R-3	N22°W	3.8 "
	R-6	N68°W	2.8 "
Donzurubo (34°32'N, 135°40'E)	E-2	E04.5°S	3.9×10^{-9} /mm
	R-2	E04.5°S	2.7×10^{-8} /mm
	R-3	N04.5°E	2.8 "
	R-6	N40.5°W	2.0 "

(3) Frequent earthquakes have occurred concentrically in this narrow zone that is the "Yodo River Seismically Active Zone", so, numerous data can be easily obtained within a short period of observations.

2. Observation Stations and Instruments

The data used in this paper have been obtained from records of the roller type super-invar bar extensometers installed at the Iwakura, Amagase and Donzurubo Observatories. The locations of these Observatories are shown in Fig. 1. The standards of length are composed of about 2~44 meters. The longest extensometer, at the Donzurubo Observatory (44 m), is capable of detecting the strain of the order of 10^{-9} , and the shortest extensometer, at the Iwakura Observatory (2m), is of the order of 10^{-7} .

The sensitivities and directions of these extensometers are shown in Table 1.

Tests to examine the stability of these instruments for vibrations have been performed in the following ways using the long extensometer at the Amagase Observatory (40 m); (1) repeated loading and unloading of a 100 g lead weight upon any intermediate part of the standard bar; (2) giving several raps on the bar with fingers or with a hammer. Fig. 2 shows how to perform these tests and Fig. 3 also shows some examples of records of these tests. From these tests, it has been concluded that the roller type super-invar bar extensometer was fairly stable for abrupt vibrations induced by external forces.

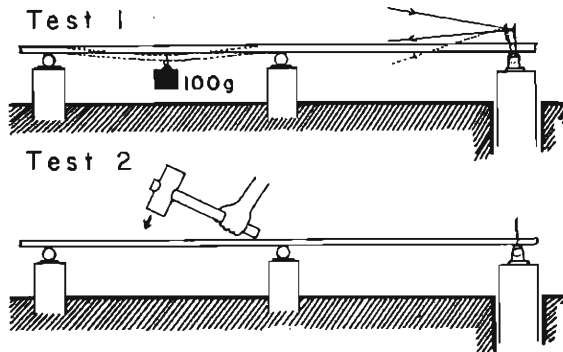


Fig. 2 Methods of experiments to examine the stability of instruments.

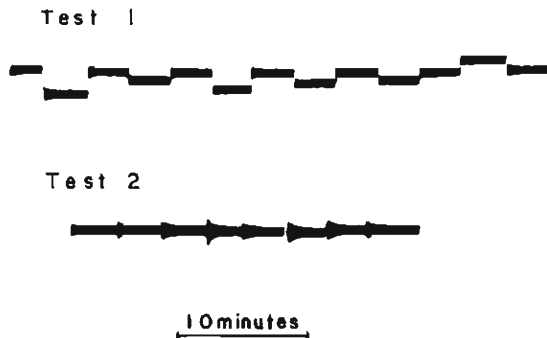


Fig. 3 Examples of records of experiments obtained at the Amagase observatory.

3. Strian Step Amplitude Related to Magnitude and Distance

Fig. 4 — (a), (b), (c) show examples of strain step records obtained at the Iwakura, Amagase and Donzurubo Observatories with super-invar bar extensometers for the earthquake of magnitude 5.6 which occurred on Aug. 18, 1968 near Wachi, in the middle part of Kyoto Prefecture.

A summary of all the data of strain steps which were obtained at the three Observatories from June 1966 to September 1968 for 163 shallow earthquakes occurring in and near Japan with a magnitude greater than 6, and for 29 local earthquakes occurring in the Yodo River Seismically Active Zone ($3.2 \leq M \leq 5.6$) is shown in Fig. 5.

Considering the detection ability of the instruments, it is precisely determined whether strain steps larger than 10^{-8} existed or not. Now, if (M) is the smallest earthquake magnitude from which strain steps of the order of 10^{-8} may be expected at a distance of R km, the empirical relationship between (M) and (R) can be obtained as a following form,

$$M = 2.2 \log R - 10.6. \quad (1)$$

Similar relationships between (M) and (R) for strains of the order of 10^{-7} and 10^{-9} can be obtained with the same slope as the 10^{-8} contour, when these contours are at regular intervals.

Assuming that the residual strain amplitude ϵ decays with $R^{-\alpha}$, where R is the epicentral distance, we obtain $\alpha = 2.4$ by taking a cross section of Fig. 5 for the same magnitude,

$$\epsilon \propto R^{-2.4}. \quad (2)$$

Similar observations of strain steps by Wideman and Major suggested the empirical value of $\alpha = 1.5$. On the other hand, the theoretical value of $\alpha = 3$ was proposed by

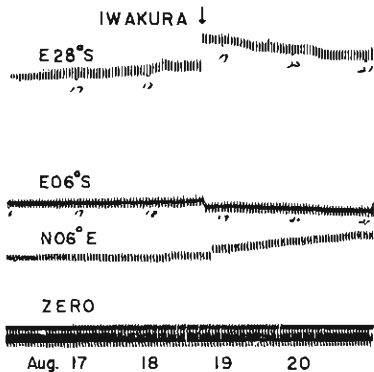


Fig. 4-(a) Strain step records obtained at the Iwakura Observatory for earthquake No. 14 ($M = 5.6$, $\Delta = 41$ km)

E28°S: -2.9×10^{-7}
 E06°S: 1.0 "
 N06°E: -2.5 "

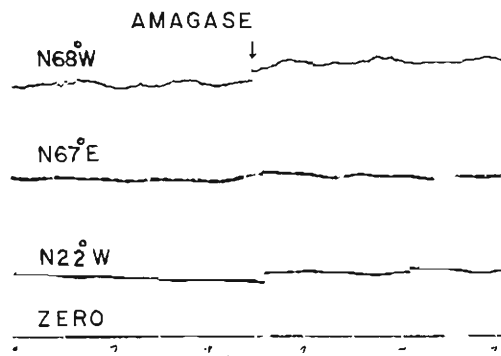


Fig. 4-(b) Strain step records obtained at the Amagase Observatory for earthquake No. 14 ($M = 5.6$, $\Delta = 57$ km)

N68°W: -1.8×10^{-8}
 N67°E: -0.4 "
 N22°W: -1.1×10^{-7} .

Press (1965), based on the elasticity theory of dislocations, for a vertical, strikeslip fault in a uniform elastic halfspace model.

Ben-Menahem et al. (1969)⁷⁾ claimed that calculations of residual strain fields at a teleseismic distance based on the halfspace approximation to a spherical earth may lead to serious errors. But to discuss this problem in detail, we must wait for sufficient data.

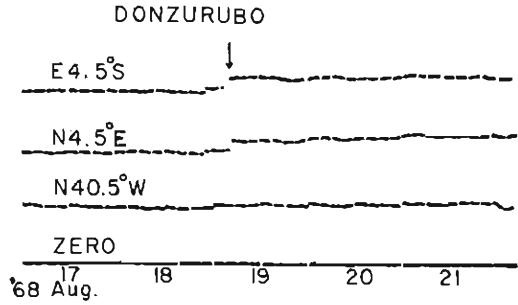


Fig. 4-(c) Strain step records obtained at the Donzurubo Observatory for earthquake No. 14 ($M=5.6$, $\Delta=80$ km)
 E04.5°S : -7.4×10^{-8}
 N04.5°E : -8.1 "
 N40.5°W : $0 (< 5 \times 10^{-9})$.

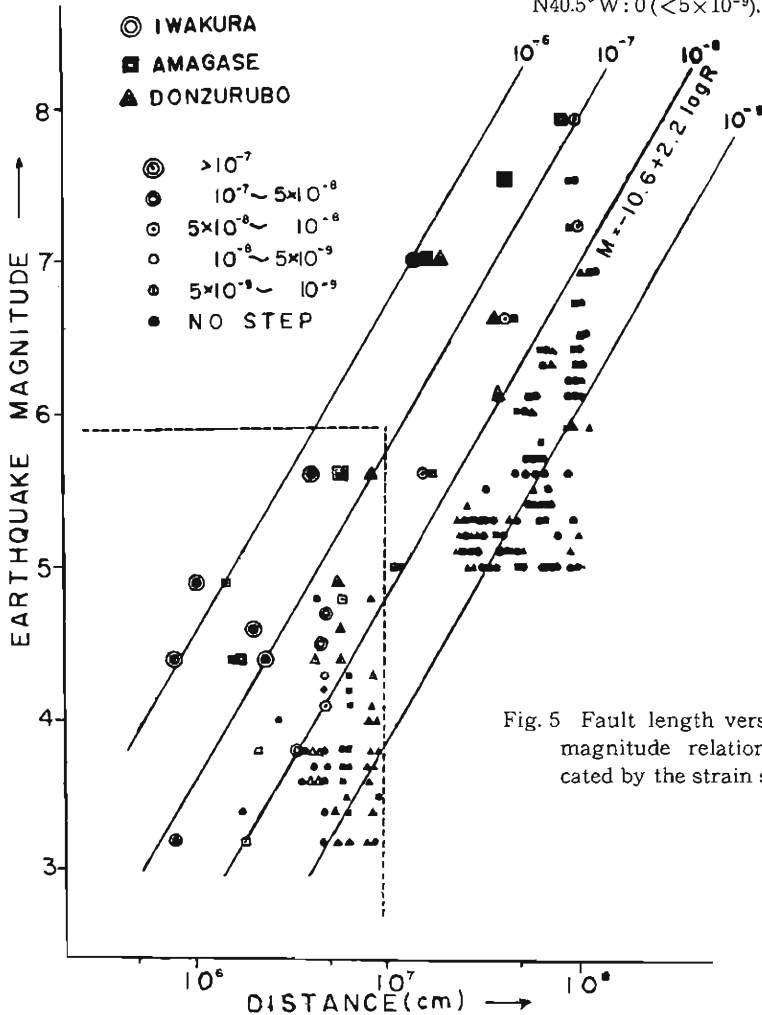


Fig. 5 Fault length versus earthquake magnitude relationship as indicated by the strain step amplitude.

4. Assumed Fault Length and Earthquake Magnitude

The ultimate strain of the earth's crust has been considered to be of the order of $10^{-4} \sim 10^{-5}$; this is based on studies of deformations of the earth's surface caused by major earthquakes, and on laboratory tests on crustal rocks (e. g. Tsuboi, 1956⁸⁾).

Let us assume that the empirical value of $\alpha=2.4$ which was obtained with super-invar bar extensometers for strains of the order of $10^{-7} \sim 10^{-9}$ can be extrapolated for all fields of residual strains caused by earthquakes. Let (R) be the maximum distance at which strains of the order of 10^{-8} may be expected; and let (R_0) be the half length of the fracture zone. The ratio of (R/R_0) can be computed as follows when the ultimate strain of the earth's crust has been assumed to be of the order of 10^{-4} , $10^{-4.5}$ and 10^{-5} respectively,

The ultimate strain	(R/R_0)
10^{-4}	46
$10^{-4.5}$	29
10^{-5}	13

On the other hand, Press's contour maps, showing relative strain as a function of fault length, indicated that strains of the order of 10^{-8} may be expected at a distance of at the most 10 fault lengths from the epicenters of earthquakes, that is, $R \approx 10 L$.

Now, the half length of the fracture zone (R_0), defined above, is considered to be the same as the semi-length dislocation surface ($1/2 L$). So it is adequate to take $R = 10 L (= 20 R_0)$.

After substituting the value of $R = 10 L$ in eq. (1), we obtain the following relationship between the assumed fault length (L) and the earthquake magnitude (M):

$$M = 2.2 \log L - 8.4 \quad (3)$$

Several authors have found approximate correlations between the fault length (L) and the earthquake magnitude (M) for shallow earthquakes. The first investigation of this type was reported by Tocher (1958)⁹⁾ for the California and Nevada shocks with a magnitude greater than 6.3. Iida (1959, 1965)^{10, 11)} has also investigated about 60 earthquakes occurring worldwide, and the following relations have been proposed:

$$M = 0.98 \log L + 0.75 \quad (\text{Tocher})$$

$$M = 0.76 \log L + 2.27 \quad (\text{Iida})$$

Otsuka (1965)¹²⁾ considered that an upper limit of fault length had to exist for each magnitude, because the strain energy accumulation per unit volume of material of the earth's crust is more or less invariable and therefore the site of storage of a limited amount of energy corresponding to that magnitude could not be indefinite; using data supplied by Iida he obtained the relationship between the maximum fault length (L_{max}) and the earthquake magnitude (M) as the following:

$$M = 2 \log L_{\text{max}} - 6.4. \quad (\text{Otsuka})$$

Wyss and Brune (1968)¹³⁾ attempted to relate the square root of the fault plane area (A) instead of the fault length (L) to the earthquake magnitude (M) for earthquakes

occurring in the California-Nevada region including earthquakes of as relatively small magnitude as $M=3.0$;

$$M=1.9 \log A^{\frac{1}{2}} - 6.7. \quad (\text{Wyss and Brune})$$

Comparing equation (3) with other empirical relationships, we find it in disagreement with the results obtained by Tocher and Iida, which have been obtained by using the data of visible seismic faultings caused by major earthquakes; but it in fair agreement with the results obtained by Otsuka, and Wyss and Brune. It is also shown in Fig. 6 that eq. (3) warps roughly the maximum values of the observed fault lengths for each magnitude. This is reasonable because eq. (3) has not been obtained from data of actual seismic faultings observed on the earth's surface but has been estimated using strain step data observed with extensometers.

Furthermore, combining eq. (3) with Gutenberg-Richter's formula of earthquake energy (E),

$$\log E=11.8+1.5M, \quad (4)$$

it is interesting that earthquake energy (E) seems to be proportional to $L^{3.3}$. This fact supports the volumical storage of earthquake energy.

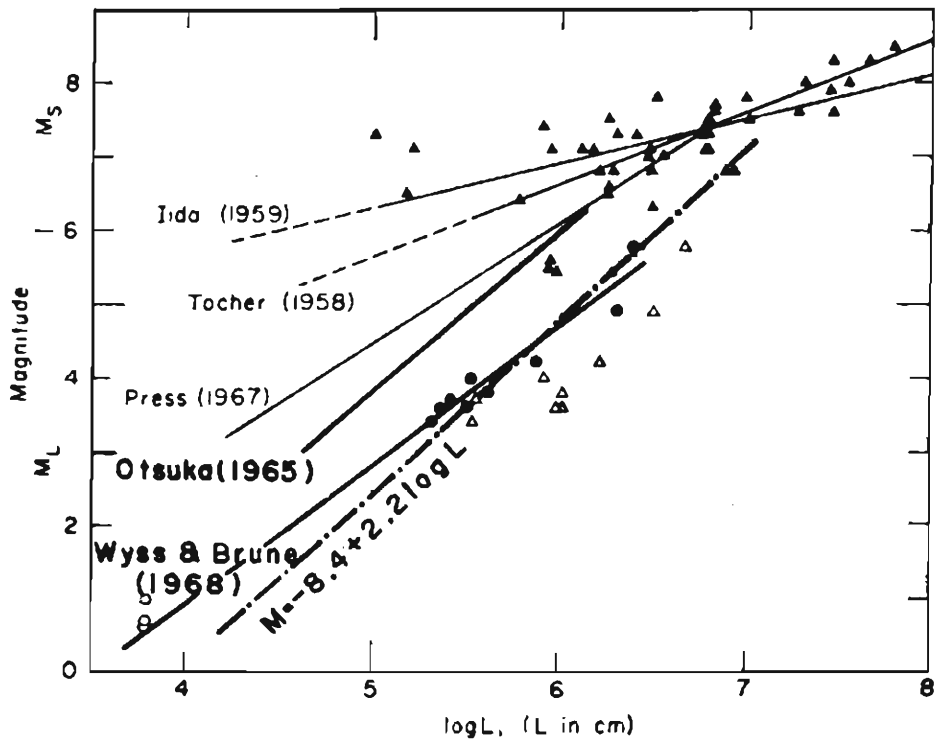


Fig. 6 Earthquake magnitude versus fault length (after Wyss and Brune).

5. Strain Steps and the Dislocation Fault Model

The distribution of epicenters determined by the J.M.A. for 29 local earthquakes occurring in the northern part of the Kinki district, the Yodo River Seismically Active Zone, from June, 1966 to September, 1968 is shown in Fig. 1 and Table 2.

According to Okano and Hirano⁵⁾, this belt-like seismically active zone lies on the right bank of the Yodo river and the push-pull distribution of the first *P*-waves of micro-earthquakes occurring in this zone is approximated by a quadrant type with two nodal lines crossing each other perpendicularly and the horizontal component of the maximum pressure is considered to lie in the E—W direction.

This direction of the maximum pressure agrees fairly well with that of the shallow

Table 2

No.	Date	Origin Time (J. S. T.)	Mag.	Lat.	Long.
		h m s			
1	15 June '66	17 30 39.4	4.5	34°56'N	135°21'E
2	29 June	21 21 56.8	4.7	34 47	135 24
3	3 Oct.	05 31 27.9	3.8	34 53	135 31
4	4 Nov.	05 39 02.2	3.6	34 57	135 39
5	12 Nov.	22 25 32.3	4.0	35 19	135 40
6	29 Mar. '67	16 46 03.2	3.2	34 40	135 01
7	10 Apr.	23 47 17.1	3.5	34 33	135 01
8	27 Apr.	14 41 32.6	3.6	34 51	135 31
9	21 June	21 09 51.2	4.6	35 02	135 35
10	1 July	19 05 27.3	3.8	34 53	135 26
11	4 Nov.	08 09 50.1	3.4	35 01	135 37
12	20 Jan. '68	11 31 37.0	4.4	34 55	135 39
13	14 Feb.	11 31 25.8	4.8	35 13	135 21
14	18 Aug.	16 12 13.3	5.6	35 13	135 23
15	18 Aug.	18 05 28.9	3.4	35 14	135 18
16	18 Aug.	21 04 04.8	3.5	35 12	135 18
17	21 Aug.	07 43 45.3	3.7	35 12	135 21
18	23 Aug.	16 24 53.0	3.8	35 15	135 20
19	27 Aug.	21 58 43.7	4.9	35 00	135 45
20	27 Aug.	22 52 53.6	4.4	35 01	135 46
21	28 Aug.	16 21 20.9	3.6	35 11	135 18
22	31 Aug.	11 14 08.6	4.3	35 14	135 19
23	3 Sep.	03 41 56.6	3.2	35 02	135 45
24	3 Sep.	06 18 24.6	3.8	35 12	135 20
25	4 Sep.	00 00 38.6	3.7	35 09	135 16
26	7 Sep.	01 36 12.9	4.6	35 13	135 19
27	11 Sep.	14 49 08.2	4.0	35 15	135 20
28	18 Sep.	15 46 56.9	4.2	35 14	153 20
29	19 Sep.	23 19 09.6	3.2	35 12	135 17

remarkable earthquakes which occurred in this region.

Similar conclusions were obtained by Hashizume et al.⁶⁾

For the 29 earthquakes which have been investigated in this paper, the push-pull distributions have seemed to show similar patterns as mentioned above except in a few cases.

Now, as a first approximation, accepting a vertical, strike-slip dislocation fault as a source model, we assume the strike direction of the fault plane to be N45°E for the right-lateral or N45°W for the left-lateral fault model.

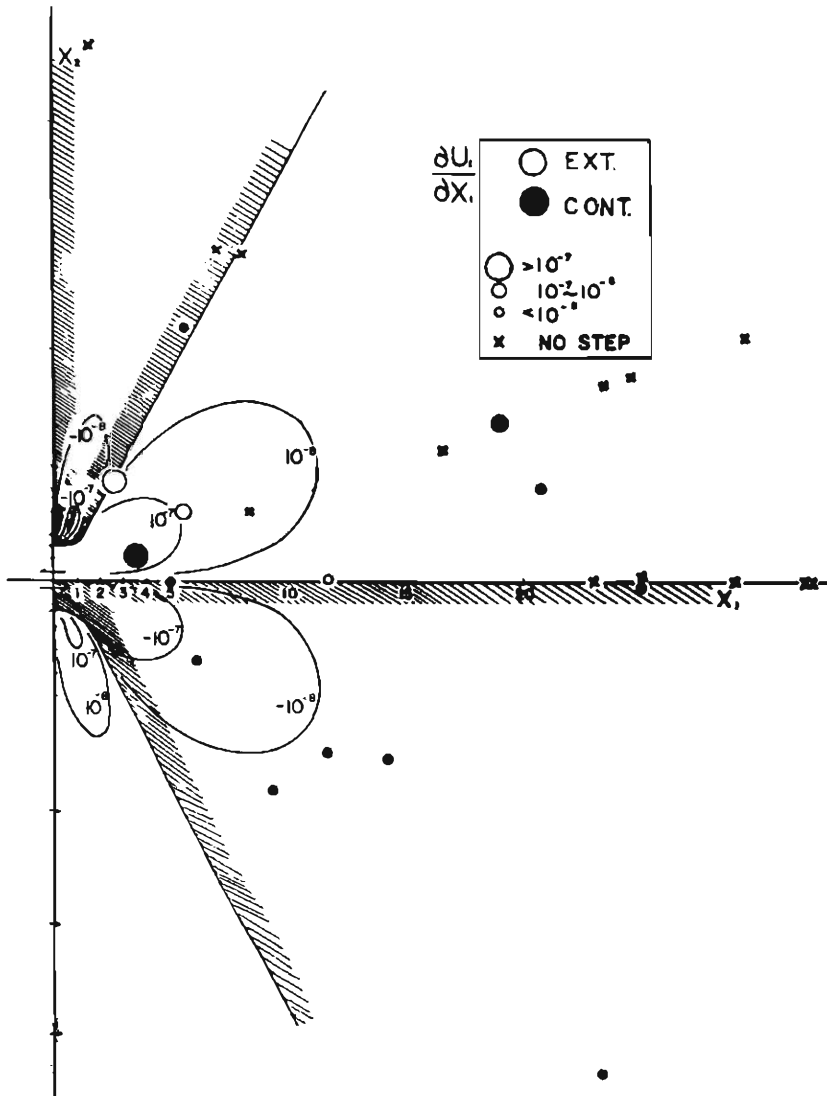


Fig. 7-(a) Observed values of strain step amplitudes and a residual strain field for strike-slip with $D=0.5L$ and $U=1/6 \times 10^{-4}L$ (X_1 -direction).

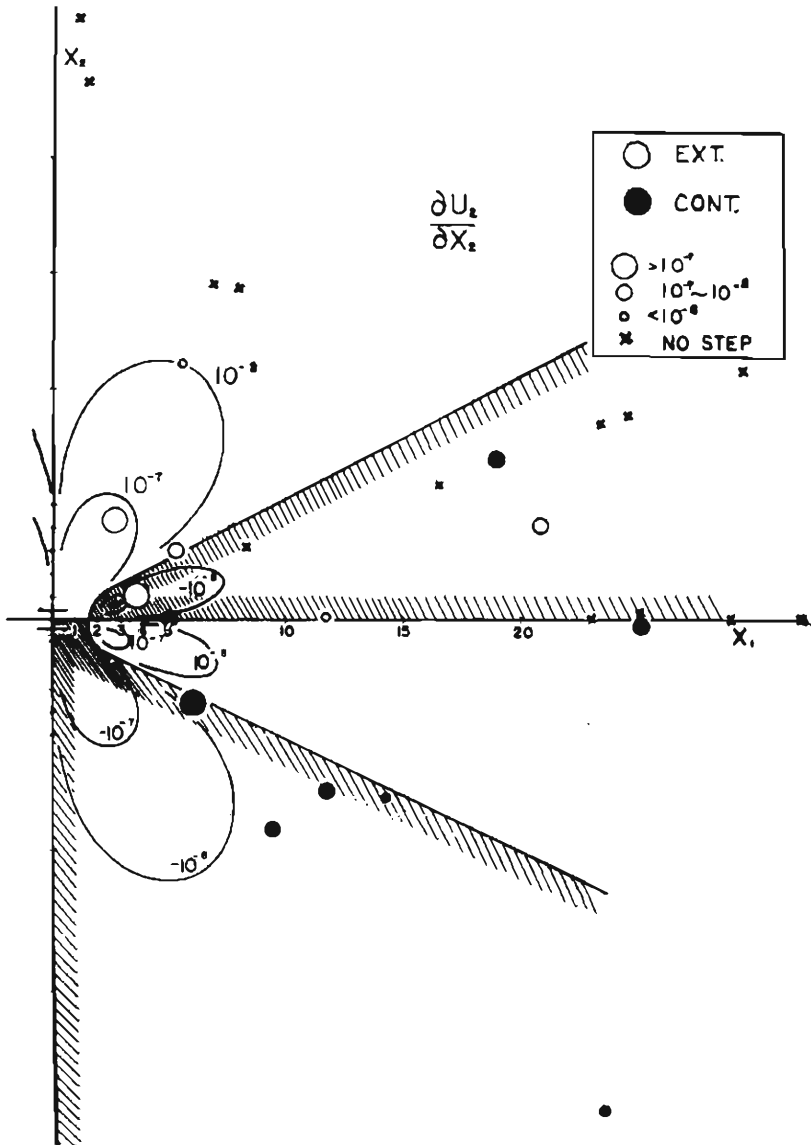


Fig. 7-(b) Observed values of strain step amplitudes and a residual strain field for strike-slip with $D=0.5 L$ and $U=1/6 \times 10^{-4} L$ (X_2 -direction).

Fig. 7-(a), (b) show the observed strain step amplitudes for the directions parallel and perpendicular to the fault strike in connection with the contour maps of residual strain fields calculated by Press for a vertical, strike-slip fault in an elastic half-space model. In these figures, the data of strain steps obtained at the three observatories, using super-invar bar extensometers, have been normalized and superposed with eq. (3) as a function of the fault length.

In regard to other fault parameters, i. e. the fault width (D) and the relative displacement (U), we had nothing to determine these values. Here, Press computed them for the two cases of $D=0.5 L$, $U=1/6 \times 10^{-4} L$ and $D=0.05 L$, $U=1/6 \times 10^{-4} L$. Since the order of observed strain step amplitudes seemed closer to the former than to the latter, we assumed it to be $D=0.5 L$ and $U=1/6 \times 10^{-4} L$. That is to say the fault width is not so thin in comparison with the fault length, but is of comparable order.

The observed values are in fair agreement with the theoretically computed contours except in a few cases. These exceptions are the values obtained at the Iwakura Observatory for earthquakes No. 14 and No. 26, and the value from the Amagase Observatory for earthquake No. 11. The latter two earthquakes were comparatively small and the amplitudes of the observed strain steps were not so significant; but earthquake No. 14 was the largest shock that occurred in this region during the observation period, and the observations were carefully made. So, a detailed consideration must be made of this disagreement.

Fig. 8 shows the distribution of the first P -waves of this earthquake (personal communication from A. Kuroiso). The directions of the nodal lines of this earthquake are different by about 10° anticlockwise from those accepted as a first approximation.

After correcting the direction of the fault strike, we again compared the observed values of the strain steps with the theoretical ones. But we could not obtain good agreement between them.

However, in this region, there has existed a clear left-lateral strike-slip fault which was discovered by Huzita¹⁴⁾ using topographical and geomorphological methods. He found that the fault strike ran along the NWW-SEE direction and that this fault system extended for about 10 km, and he named it the Mitoke Fault. Fig. 9 shows a detailed discription of the Mitoke Fault as well as the epicenters of the main shock (No. 14), a foreshock (No. 13) and a remarkable aftershock (No. 22) which were determined independently by the Abuyama Seismological Observatory and the J.M.A. The epicenters of these earthquakes lay just on the branch of the Mitoke Fault, therefore it is reasonable to consider that these earthquakes are closely related to this Mitoke Fault.

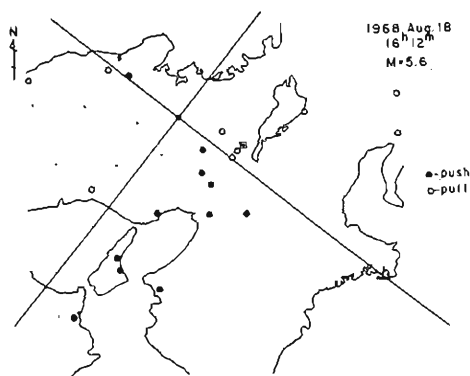


Fig. 8 Distribution of the first P -wave motions of No. 14 earthquake
 ●: Push, ○: Pull, ■: the Iwakura Obs..

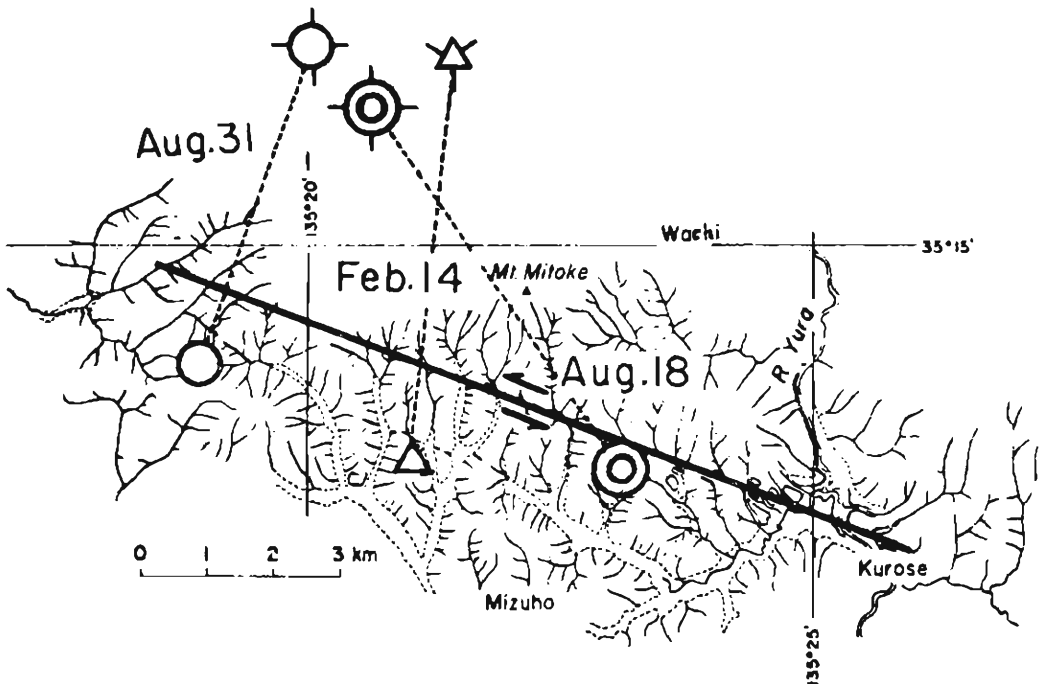


Fig. 9 Map of the left-lateral strike-slip movement along the Mitoke fault (after Huzita) and locations of epicenters.

⊙, ○, △: the J. M. A.
 ⊕, ⊖, ✕: the Abuyama Seismological Observatory

If we modify the azimuth of the fault strike of this earthquake (No. 14) to a direction coincident with that of the Mitoke Fault, we can obtain good agreement between the observed and the theoretical values. In this case, other observed values obtained at the Amagase and Donzurubo Observatories were not incompatible with the theoretical ones.

But there was one more assumption in the process of obtaining Press's contour maps of residual strain fields; the relative displacement (U) had to be equal to $1/6 \times 10^{-4} L$, where (L) was the fault length. So, we have checked up the relationship between (U) and (L) using the table given by King and Knopoff¹⁵⁾ for strike-slip faults.

Fig. 10 shows (U) plotted against (L) based on this table. In the case of larger earthquakes ($M \geq 6.0$), it appears that the (U)-values plotted against (L) lie almost between two straight lines, $U=10^{-4} L$ and $U=10^{-5} L$. But for smaller earthquakes ($M < 6.0$), although only two examples are listed in the table, i.e. the cases of the Parkfield earthquake ($M=5.6$) and the Imperial earthquake ($M=3.6$), the U - L relationship is different from that for the larger earthquakes and it seems to be $U < 10^{-5} L$. However, Aki¹⁶⁾ has estimated the relative displacement (U) for the Parkfield earthquake as 60 cm, using the data of the accelograms obtained only 80 m from the San Andreas Fault, and this value was one order larger than that obtained from field observations. He explained that this disagreement was caused by the decoupling layer near the surface. If this is true, the (U)-value plotted against (L) for the

Parkfield earthquake is expressed by (4) in Fig. 10 and for the smaller earthquakes, too, the following relationship can be considered between (U) and (L):

$$U = (10^{-4} \sim 10^{-5}) \times L \tag{5}$$

Therefore, the assumption of $U = 1/6 \times 10^{-4} L$ may be not so irrelevant.

In conclusion, strain steps associated with local earthquakes which have not been accompanied with visible seismic faultings can be explained well with the dislocation fault model. In this case, the assumed fault width is not so thin in comparison with the fault length but is of a comparable order, and the values of $D = 0.5L$ and $U = (10^{-4} \sim 10^{-5}) \times L$ are compatible with the data of strain steps.

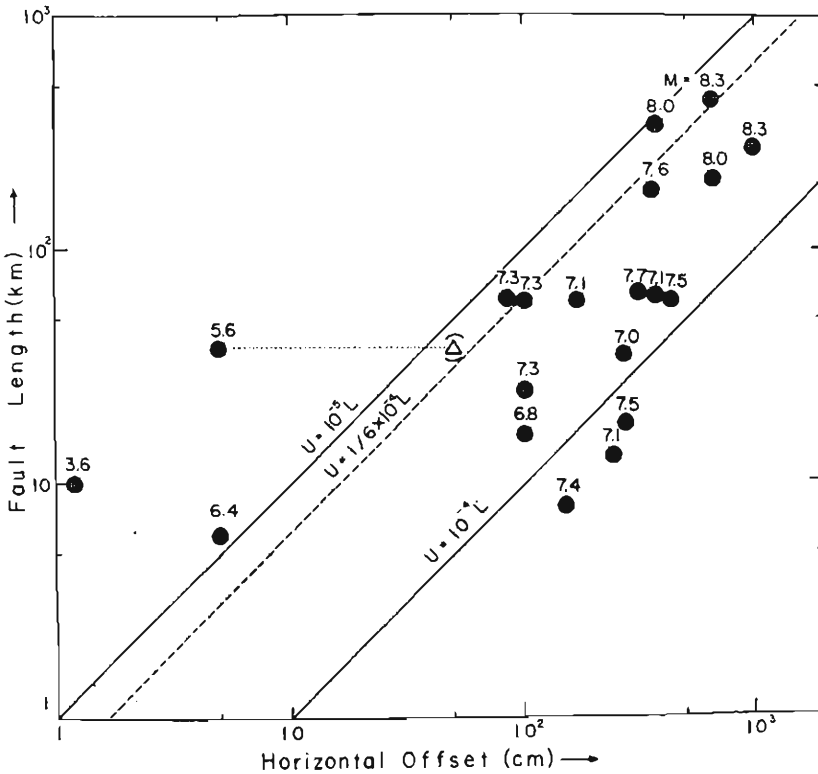


Fig. 10 Strike-slip fault length versus horizontal offset.

6. Some Implications in the Seismic Moment

The seismic moment as a function of an earthquake's magnitude was first estimated by Brune¹⁷⁾ in order to calculate rates of slip along major faults. Further, Wyss and Brune¹³⁾, using the analysis of surface waves, obtained the following moment-versus-magnitude relations,

for the Parkfield region

$$\log M_0 = 1.4M_L + 17.0 \quad (3 < M_L < 6)$$

for the western United States

$$\log M_0 = 1.7M_L + 15.1 \quad (3 < M_L < 6)$$

where (M_0) is the seismic moment and (M_L) is the Richter magnitude.

According to the elasticity theory of dislocations, the seismic moment (M_0) is proportional to the product of the average dislocation (U) times the area of the dislocation ($L \times D$),

$$M_0 = \mu U(L \times D) \quad (6)$$

where μ is the rigidity.

Substituting $U = (10^{-4} \sim 10^{-5}) \times L$, $D = 0.5L$ and $\mu = 3 \times 10^{11}$ into eq. (6), we have

$$M_0 = 1.5 \times (10^7 \sim 10^6) \times L^3 \quad (7)$$

and from the magnitude—fault length relationship of eq. (3) in conjunction with eq. (7), we have a following expression for earthquakes occurring in the northern part of the Kinki district.

$$\log M_0 = 1.4M + (18.7 \sim 17.7) \quad (3 < M < 6) \quad (8)$$

In eq. (8), the estimated value of the seismic moment for each magnitude is about one order larger than that obtained by Wyss and Brune for the California-Nevada earthquakes.

This discrepancy may be attributed to over-estimating the average dislocation (U). And these calculations have been based on a few rough assumptions and are not suitable for detailed discussion.

7. Concluding Remarks

Strain steps observed with roller type super-inver bar extensometers seem to represent the static residual strains caused by earthquakes. The amplitude of strain step decays with distance of $R^{-2.4}$ and the following empirical relationship between (M) and (R) has been derived:

$$M = 2.2 \log R - 10.6$$

where (M) is the smallest earthquake magnitude from which a strain step of the order of 10^{-8} may be expected at a distance of R km.

Assuming that residual strains of the order of 10^{-8} are observed at distances of 10 fault lengths, the following relationship between the earthquake magnitude (M) and the fault length (L) can be obtained,

$$M = 2.2 \log L - 8.4.$$

Further, for 29 local earthquakes which were not accompanied with visible seismic faultings on the earth's surface, the observed strain steps could be well explained with the dislocation fault model.

Concerning the seismic moment (M_0), we obtained the following tentative relationship,

$$\log M_0 = 1.4M + (18.7 \sim 17.7).$$

But detailed discussion must wait for more data; and it is also necessary to study this problem from other points of view using the data of seismographs and geodetic surveys.

The author wishes to express his thanks to Prof. Michio Takada for his kind guidance and to Dr. Torao Tanaka and Mr. Tamotsu Furuzawa for their comments. Thanks are also due to Mr. Kensuke Onoue and to Mr. Masaru Yamada for their help concerning the observations.

References

- 1) Chinnery, M. A.: The Deformation of the Ground Around Surface Faults, *Bull. Seism. Soc. Am.*, Vol. 51, 1961, pp. 355-372.
- 2) Press, F.: Displacements, Strains, and Tilts at Teleseismic Distances, *J. Geophys. Res.*, Vol. 70, 1965, pp. 2395-2412.
- 3) Wideman, C. J. and M. W. Major: Strain Steps Associated with Earthquakes, *Bull. Seism. Soc. Am.*, Vol. 57, 1967, pp. 1429-1444.
- 4) Okano, K. and I. Hirano: Earthquakes Occurring in the Vicinity of Kyoto, *J. Phys. Earth*, Vol. 16, 1968, pp. 141-152.
- 5) Okano, K. and I. Hirano: Micro-earthquakes Occurring in the Vicinity of Kyoto (2), *Annuals, Dis. Prev. Res. Inst., Kyoto Univ.*, No. 9, 1966, pp. 21-26.
- 6) Hashizume, M. et al.: Investigation of Micro-earthquakes in Kinki District—Seismicity and mechanism of their occurrence—, *Bull. Dis. Prev. Res. Inst.*, Vol. 15, part 3, 1966, pp. 35-48.
- 7) Ben-Menahem, A. et al.: Static Deformation of a Spherical Earth Model by Internal Dislocations, *Bull. Seism. Soc. Am.*, Vol. 59, 1969, pp. 813-853.
- 8) Tsuboi, T.: Earthquake Energy, Earthquake Volume, Aftershock Area, and Strength of the Earth's Crust, *J. Phys. Earth*, Vol. 4, 1956, pp. 63-66.
- 9) Tocher, D.: Earthquake Energy and Ground Breakage, *Bull. Seism. Soc. Am.*, Vol. 48, 1958, pp. 147-153.
- 10) Iida, K.: Earthquake Energy and Earthquake Fault, *J. Earth Sci., Nagoya Univ.*, Vol. 7, 1959, pp. 98-107.
- 11) Iida, K.: Earthquake Magnitude, Earthquake Fault and Source Dimensions, *ibid.*, Vol. 13, 1965, pp. 115-132.
- 12) Otsuka, M.: Earthquake Magnitude and Surface Fault Formation, *Zisin*, Vol. 18, 1965, pp. 1-8.
- 13) Wyss, M. and J. N. Brune: Seismic Moment, Stress, and Source Dimensions for Earthquakes in the California-Nevada Region, *J. Geophys. Res.*, Vol. 73, 1968, pp. 4681-4694.
- 14) Huzita, K.: Tectonic Development of Southwest Japan in the Quaternary Period, *J. Geosci., Osaka City Univ.*, Vol. 12, 1969, pp. 53-70.
- 15) King, Chi-Yu, and L. Knopoff: Stress Drop in Earthquakes, *Bull. Seism. Soc. Am.*, 1968, pp. 249-257.
- 16) Brune, J. N.: Seismic Moment, Seismicity and Rate of Slip Along Major Fault Zones, *J. Geophys. Res.* Vol. 73, 1968, pp. 777-784.